RAPID COMMUNICATION

Magneto-volume effect in Fe_nTi_{13-n} clusters during thermal expansion

Jian Huang(黄建), Yanyan Jiang(蒋妍彦), Zhichao Li(李志超),
Di Zhang(张迪), Junping Qian(钱俊平), and Hui Li(李辉)†

Key Laboratory for Liquid-Solid Structural Evolution and Processing of Materials, Ministry of Education, Shandong University, Jinan 250061, *China*

(Received 17 August 2022; revised manuscript received 28 December 2022; accepted manuscript online 30 December 2022)

Ab initio molecular dynamics calculations have been carried out to search for the ground state structure of Fe_nTi_{13-n} clusters and measure the thermal expansion of Fe_nTi_{13-n}. The volume of Fe_nTi_{13-n} clusters during thermal expansion is jointly determined by anharmonic interaction and magneto-volume effect. It has been found that Fe_6Ti_7, Fe_9Ti_4, $Fe_{11}Ti_2$, and Fe_{13} clusters can exhibit the remarkable magneto-volume effect with abnormal volume behaviors and magnetic moment behaviors during thermal expansion. A prerequisite for the magneto-volume effect of Fe_nTi_{13-n} clusters during thermal expansion has been revealed and the magnitude of the magneto-volume is also approximately determined. Furthermore, the magneto-volume behaviors of Fe_nTi_{13-n} clusters are qualitatively characterized by the energy contour map. Our results shed light on the mechanism of the magneto-volume effect in Fe_nTi_{13-n} clusters during thermal expansion, which can guide the design of nanomaterials with zero expansion or even controllable expansion properties.

Keywords: Fe_nTi_{13-n} cluster, thermal expansion, magneto-volume effect, magnetic moment

PACS: 65.40.De **DOI:** 10.1088/1674-1056/acaf2e

1. Introduction

The magneto-volume effect,[1] which refers to the interaction between magnetic transition and volume change of materials,[2] has been the subject of extensive research over the past decades. There are a multitude of physical phenomena and applications associated with the magneto-volume effect, such as Invar alloys and antiperovskite materials with negative thermal expansion. The origin of the Invar effect in low expansion alloys is still controversial,[3] but it has been widely accepted that it is tightly connected to the existence of different magnetic states with different volumes,[4–8] and the transition between them would lead to the suppression of thermal expansion. The spontaneous volume magnetostriction of ferromagnetic transition metals at the Curie temperature is produced by the transition from the ferromagnetic state to the paramagnetic state.[9,10] Antiferromagnetic antiperovskite materials such as $Mn_3Cu_{1-x}Ge_xN$ exhibit negative thermal expansion over a certain temperature range due to the transition from the antiferromagnetic state to the paramagnetic state with the temperature increasing.[11–14] These volume change behaviors contradict the traditional pattern of thermal expansion and cold contraction caused by the anharmonic lattice vibration.[15,16] Since these phenomena are all owing to the magnetic transition of materials induced by the temperature, it is considered as the magneto-volume effect. Previous studies have shown that the magneto-volume effect can be contributed by the transition from the magnetic order state to the paramagnetic state,[17–24] the transition between the ferromagnetic state and the antiferromagnetic state,[25,26] the change of local magnetic moment,[4,27,28] and so on.

Clusters have very different properties from bulk. Plenty of efforts have been devoted to studying the magneto-volume effect of bulk materials, while studies focusing on the thermal expansion of clusters are scarce.[29] Exploring the magneto-volume effect at the cluster scale is of great significance for further understanding it. In this paper, we mainly concentrate on the thermal expansion of 13-atom Fe–Ti clusters and the magneto-volume effect at the cluster scale.

2. Computational methods

Our first-principles calculations, mainly including geometry optimization, static calculation, and *ab initio* molecular dynamics (AIMD) calculation, are performed using density functional theory (DFT) implemented in the Vienna *ab initio* simulation package (VASP).[30–33] The exchange–correlation energy functional is described by the Perdew–Burke–Ernzerhof (PBE) method based on the generalized gradient approximation (GGA).[34,35] The projected augmented wave (PAW) method is adopted.[36] For all calculations, the cutoff energy for the plane-wave basis set is 300 eV. The total energy is converged to less than 10^{-4} eV/atom, while the atomic force is converged to less than 0.01 eV/Å. We perform all calculations using a single k point (Γ point) for the Brillouin-zone integration, and we use a cubic simulation box with a lattice parameter of 20 Å. For AIMD calculations, the canonical ensemble (NVT) is employed with the Nose–

†Corresponding author. E-mail: lihuilmy@hotmail.com

© 2023 Chinese Physical Society and IOP Publishing Ltd

Hoover thermostat.[37,38] to control the temperature, with a time step of 1 fs.

It is well known that even a simple Fe_{13} cluster contains thousands of local energy minimum configurations.[39] Although it is difficult to determine the ground state structure of Fe_nTi_{13-n}, there are three common methods. The first is the annealing method.[40,41] where the clusters are relaxed at 3000 K to obtain the disordered structures, and then cooled to 0 K to acquire the annealed structures. The second approach is the relaxation method,[42] which relaxes the disordered clusters at 1000 K, and then searches for several structures corresponding to the minimum values on the potential energy surface. After optimizing the selected structures, the most stable configuration is determined. The third one is the prediction method.[43] Previous research has shown that the ground state structures of Fe_{13} and Ti_{13} are both icosahedral structures,[43–48] so the icosahedron is relatively more stable for Fe_nTi_{13-n}. Here, according to the relative positions of Fe atoms and Ti atoms in Fe_nTi_{13-n} obtained by the annealing and relaxation methods, we set the icosahedral structure of Fe_nTi_{13-n}, and then we compare the optimized results with those obtained by annealing and relaxation to determine the ground state structure of each cluster. Three distinct structures of Fe_nTi_{13-n} clusters are produced, which are shown in supporting information.

After acquiring the ground state structure, AIMD calculations are employed to measure the thermal expansion property of Fe_nTi_{13-n} ($n = 0$, 1, 2, 6, 7, 9, 11, 12, 13) at six different temperatures: 300 K, 400 K, 500 K, 600 K, 700 K, and 800 K. Fe_nTi_{13-n} is put at a constant temperature to relax for 5000 steps with spin polarized calculation. To keep the total magnetic moment of Fe_nTi_{13-n} fixed during thermal expansion, we innovatively apply the fixed spin moment (FSM) setting to AIMD, namely, the fixed spin moment *ab initio* molecular dynamics (FSM-AIMD) calculation. Fe_nTi_{13-n} is placed at 300 K, 500 K, and 800 K to relax for 5000 steps, respectively, while keeping the difference between the number of electrons in the up and down spin components fixed by the VASP code. Actually, the ground state structures of Fe_nTi_{13-n} clusters are all close to regular or irregular icosahedrons. Therefore, we adopt the volume of the icosahedron composed by the centers of 12 atoms on the cluster surface as the volume of Fe_nTi_{13-n} clusters. Meanwhile, Fe_nTi_{13-n} clusters can still maintain the icosahedron-like structure at a particular temperature during the AIMD simulation due to the stability of icosahedron. Therefore, we employ the above-mentioned volume definition method to calculate the cluster volume corresponding to each step in the MD trajectory and take the average volume of the last 3000 steps as the cluster volume at a particular temperature.

It is well known that the GGA method cannot well describe the strong interaction of d and f electrons in transition metals. To test the accuracy of our GGA method, the GGA+U ($U = 2.5$ eV) method is applied to calculate the structural properties of Fe_2 dimer and Ti_2 dimer as shown in Table 1. It can be observed that the bond lengths of Fe_2 dimer and Ti_2 dimer calculated by the GGA+U method are both larger than the experimental data, while those calculated by the GGA method are consistent with the experimental data. Yuan *et al.*[49] have reported that the GGA+U method overestimates the spin moment of Fe_{13}^{+} cluster. Alvarado-Leyva *et al.*[50] also found that the GGA+U method would give a quite large magnetic moment in the bcc bulk (about $2.60\mu_B$ instead of $2.21\mu_B$). Therefore, the GGA+U method might not be a suitable method to explore the properties of Fe_nTi_{13-n} clusters as compared with the GGA method. We have full confidence in the GGA method as many researches on transition metal clusters have been carried out by the GGA method in the past few decades.

Table 1. Calculated atomic bond lengths of Fe_2 dimer and Ti_2 dimer at the ground state. A value of $U = 2.5$ eV is adopted in the GGA+U method to specify the strength of the effective on-site Coulomb interactions.

	Bond length (Å)		
	GGA	GGA+U	Expt.
Fe_2	2.000	2.136	2.02 ± 0.02[51]
Ti_2	1.961	2.002	1.9422 ± 0.0008[52]

3. Results and discussion

3.1. Characteristics of Fe_nTi_{13-n}

We first present the ground state structures with the lowest energy for Fe_nTi_{13-n} clusters as shown in Fig. 1. It is observed that the majority of Fe_nTi_{13-n} configurations resemble icosahedrons, and that their central atoms are always Fe atoms (with the exception of Ti_{13} and $Fe_{12}Ti_1$). Among them, Ti_{13}, Fe_1Ti_{12}, $Fe_{12}Ti_1$, and Fe_{13} are close to regular icosahedrons with D_{5d}, I_h, D_3, and D_{5d} geometric symmetries, respectively; while Fe_2Ti_{11}, Fe_7Ti_6, Fe_9Ti_4, and $Fe_{11}Ti_2$ are irregular icosahedrons with C_{5v}, C_{2v}, C_s, and C_{2v} geometric symmetries, respectively. Fe_3Ti_{10} (C_{2v}), Fe_4Ti_9 (C_s), Fe_5Ti_8 (C_{2v}), Fe_6Ti_7 (C_s), and Fe_8Ti_5 (C_s) are three-layer structures like a distorted icosahedron being compressed along a specific direction. $Fe_{10}Ti_3$ (C_1) is a unique structure with the lowest symmetry and seems to be a twisted icosahedron.

Next, we calculate the binding energy (E_b) of Fe_nTi_{13-n}. The E_b is defined as[43,53]

$$E_b = \frac{E_{cluster} - \sum n_i E_i}{\sum n_i}, \tag{1}$$

where $E_{cluster}$ is the total energy of the cluster, n_i is the number of type i atoms in the cluster, and E_i is the energy of an isolated type i atom. The variation of E_b versus the number of Fe atoms is plotted in Fig. 2(a). It follows that with the increasing number of Fe atoms in the cluster, the E_b of Fe_nTi_{13-n} decreases initially, and then gradually rises. Specially, Fe_2Ti_{11} has the lowest E_b (−3.81 eV/atom), while Fe_{13} has the highest E_b (−3.33 eV/atom). Our results are in good agreement with those from Piotowski *et al.*,[43] as marked in Fig. 2(a).

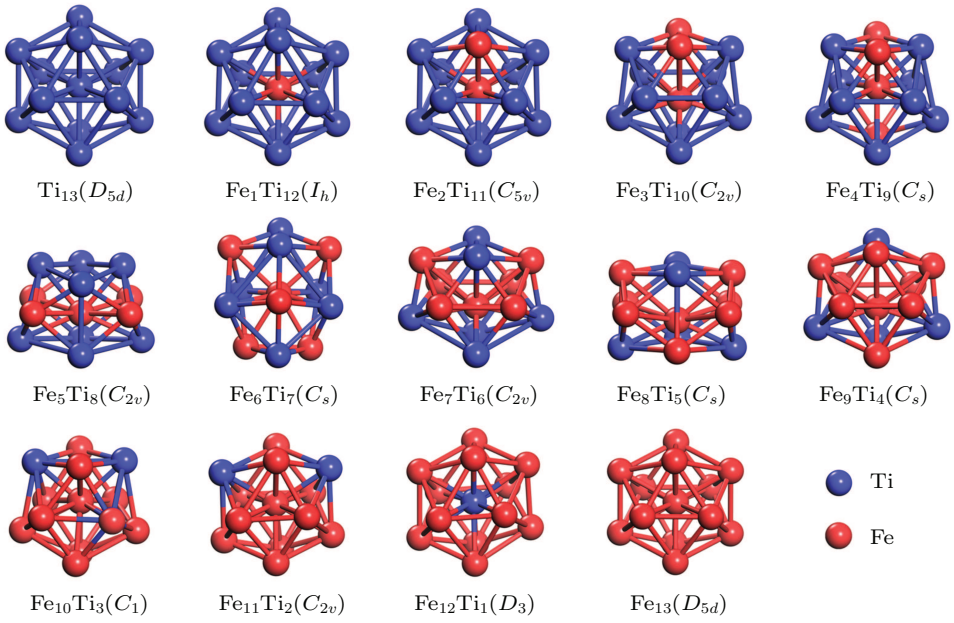


Fig. 1. Ball-and-stick models of ground state structures of the Fe_nTi_{13-n} clusters. Molecular point-group symmetries are given in parentheses with a tolerance of 0.1 Å.

Figure 2(b) shows the volume and bond length of Fe_nTi_{13-n} clusters. It is observed that the volume of Ti_{13} is the largest, with the value of around 45.6 Å^3. With the increase in the number of Fe atoms, the Fe_nTi_{13-n} volume gradually decreases and eventually swings at 35.3 Å^3. In Fe_nTi_{13-n} clusters, there are two types of chemical bonds: the chemical bonds between two surface atoms (SS bonds) and those between the central atom and surface atom (CS bonds). The bond length of Fe_nTi_{13-n} is also shown in Fig. 2(b). In general, the SS and CS bond lengths of Fe_nTi_{13-n} fluctuate and decrease as the number of Fe atoms increases, and the different ground state structures of Fe_nTi_{13-n} are thought to be the source of the bond length fluctuation. The calculated CS bond length for Fe_{13} and Ti_{13} is 2.40 Å and 2.62 Å, which are in accordance with previous work.[43,45,47,48,53,54]

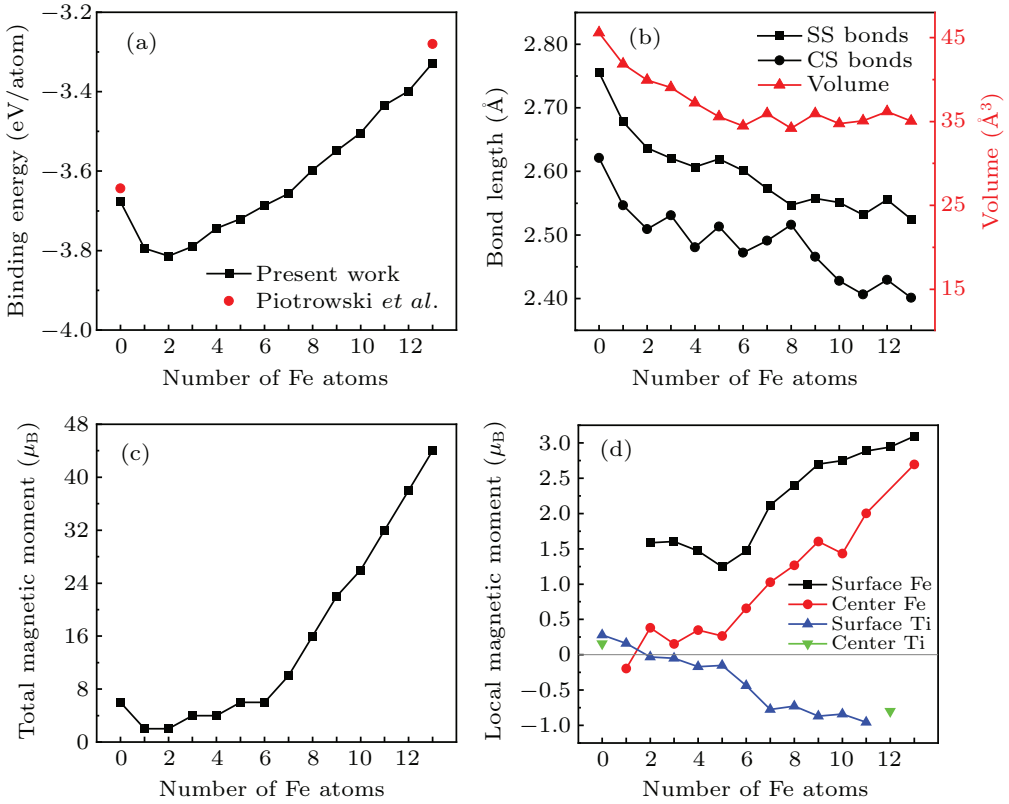


Fig. 2. The properties of Fe_nTi_{13-n} clusters. (a) The binding energy (E_b) of Fe_nTi_{13-n}. (b) The volume, CS bond length, and SS bond length of the ground state structures of Fe_nTi_{13-n}. (c) The total magnetic moment of Fe_nTi_{13-n}. (d) The local atomic magnetic moment of Fe_nTi_{13-n}.

Subsequently, the magnetism of Fe_nTi_{13-n} has been investigated, and the total magnetic moment and the local atomic magnetic moment of Fe_nTi_{13-n} are shown in Figs. 2(c) and 2(d). With the increase in the number of Fe atoms, the total magnetic moment of Fe_nTi_{13-n} fluctuates around $4\mu_B$ first and then increases sharply. Fe_{13} has the maximum magnetic moment ($44\mu_B$). For Fe atoms, the local magnetic moment is always positive, except for the center Fe atom in Fe_1Ti_{12}. The local magnetic moment of surface Fe atoms and center Fe atoms fluctuates and then rises with the increase in the number of Fe atoms, which might explain the variation trend of the total magnetic moment of Fe_nTi_{13-n}. The local magnetic moment of center Fe atoms is lower than that of surface Fe atoms, which is ascribed to the localized 3d electrons of the surface atoms.[55–57] For Ti atoms, the local magnetic moment is mainly negative, except for Ti_{13} and Fe_1Ti_{12}. It is found that only Ti_{13} and Fe_{13} exhibit ferromagnetism, while the other ones show ferrimagnetism.

3.2. Thermal expansion of Fe_nTi_{13-n}

The volume expansion ratio ($\Delta V_T/V_0$) is used to measure the thermal expansion property of Fe_nTi_{13-n} ($n = 0$, 1, 2, 6, 7, 9, 11, 12, 13), as displayed in Figs. 3(a) and 3(b). $\Delta V_T/V_0$ is calculated as $(V_T - V_0)/V_0$, where V_T represents the volume at temperature T and V_0 represents the volume of the ground state structure. The $\Delta V_T/V_0$ of Fe_nTi_{13-n} increases as the temperature rises. It is noticed that Fe_6Ti_7 has the largest $\Delta V_T/V_0$ for all temperature, followed by $Fe_{12}Ti_1$, while Fe_9Ti_4 and Fe_1Ti_{12} have relatively small $\Delta V_T/V_0$. At 300 K, the $\Delta V_T/V_0$ of Fe_9Ti_4 is about -0.06%, implying that the Fe_9Ti_4 volume at 300 K is slightly smaller than V_0. In this case, how to deal with the different $\Delta V_T/V_0$ of Fe_nTi_{13-n}? According to the E_b of Fe_nTi_{13-n} in Fig. 2(a), Fe_2Ti_{11} has the lowest E_b, while the E_b of Fe_{13} is the highest. If the $\Delta V_T/V_0$ of Fe_nTi_{13-n} is determined by the E_b, the $\Delta V_T/V_0$ of Fe_2Ti_{11} should be the smallest, and at the same time that of Fe_{13} should be the biggest, which is inconsistent with the calculation results. Therefore, the binding energy of Fe_nTi_{13-n} cannot explain the difference in the volume expansion ratio of Fe_nTi_{13-n}.

In fact, the increase in temperature not only generates the change of Fe_nTi_{13-n} volume but also leads to the shift in the spin state of Fe_nTi_{13-n} clusters manifested as the change in Fe_nTi_{13-n} total magnetic moment, as shown in Fig. 4. ΔM_T is calculated as $M_T - M_0$, where M_T represents the total magnetic moment at temperature T and M_0 represents the total magnetic moment of the ground state. As the temperature rises, the ΔM_T of Ti_{13}, Fe_1Ti_{12}, Fe_2Ti_{11}, $Fe_{11}Ti_2$, and Fe_{13} decreases, while that of Fe_6Ti_7 and Fe_7Ti_6 fluctuates around $0\mu_B$. The ΔM_T of Fe_9Ti_4 increases as the temperature rises, but it is always less than $0\mu_B$. However, the ΔM_T of $Fe_{12}Ti_1$ is always $0\mu_B$, demonstrating that the total magnetic moment of $Fe_{12}Ti_1$ always remains constant at $38\mu_B$ as temperature increases.

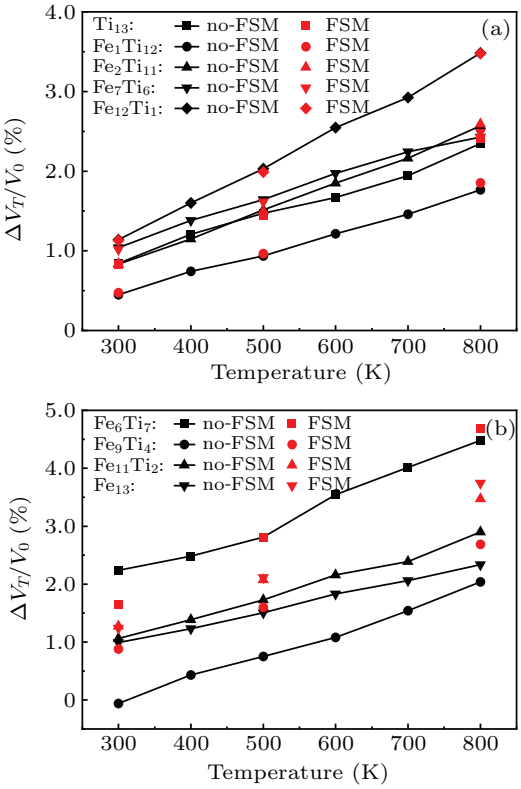


Fig. 3. Thermal expansion of Fe_nTi_{13-n} clusters. (a) The volume expansion ratio ($\Delta V_T/V$) of Fe_nTi_{13-n} ($n = 0$, 1, 2, 7, 12). (b) The volume expansion ratio ($\Delta V_T/V$) of Fe_nTi_{13-n} ($n = 6$, 9, 11, 13). The black line plot is $\Delta V_T/V$ of Fe_nTi_{13-n} calculated by AIMD without the FSM method, while the red scatter plot is $\Delta V_T/V$ of Fe_nTi_{13-n} calculated by FSM-AIMD at 300 K, 500 K, and 800 K.

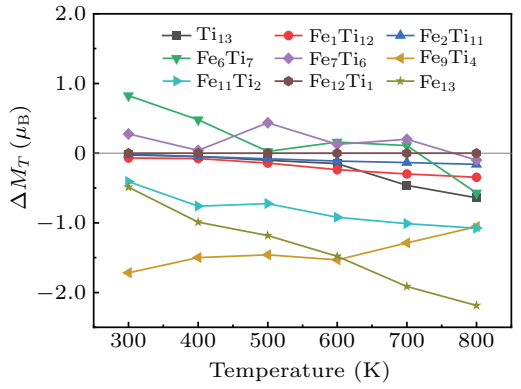


Fig. 4. The total magnetic moment difference relative to the ground state (ΔM_T) of Fe_nTi_{13-n} at different temperatures.

We have initially tried to explain the relationship among temperature, volume and total magnetic moment of Fe_nTi_{13-n} clusters during thermal expansion by using the relation in Fig. 5(a), that is, with the temperature rising, the volume will increase due to the anharmonic interaction between atoms, and the change of atomic structure of clusters will lead to the change of the total magnetic moment. Previous research[58] has demonstrated that when the volume of bcc 3d transition metals increases, so does the atom's local magnetic moment. According to the above explanation, the increasing temperature will lead to the increase of the cluster volume, and then lead to the increase of the total magnetic moment. However,

this is completely inconsistent with the actual total magnetic moment behaviors of Fe_nTi_{13-n} clusters during thermal expansion as shown in Fig. 4. Therefore, the total magnetic moment of Fe_nTi_{13-n} clusters during thermal expansion is not simply determined by the atomic structure. To better explain the relationship among temperature, volume and total magnetic moment on heating, we put forward another assumption, as shown in Fig. 5(b). When the temperature rises, the cluster volume will increase due to the anharmonic interaction, and the spin state will also shift with the temperature increasing, resulting in the change of the total magnetic moment, which further leads to the change of the cluster volume. That is to say, the volume of Fe_nTi_{13-n} clusters during thermal expansion is jointly determined by the anharmonic interaction and magneto-volume effect. Hence, we can consider the cluster volume as a binary function of temperature and total magnetic moment during thermal expansion.

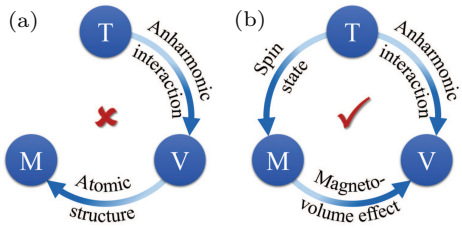


Fig. 5. Schematic illustration of the interaction of temperature, volume, and total magnetic moment of Fe_nTi_{13-n} clusters during thermal expansion. "T" represents the temperature, "V" represents the volume of Fe_nTi_{13-n} clusters, and "M" represents the total magnetic moment.

To confirm the existence of magneto-volume effect in Fe_nTi_{13-n} cluster during thermal expansion, we have simulated the thermal relaxation of Fe_nTi_{13-n} with the total magnetic moment fixed by using the FSM-AIMD calculation, ensuring that the thermal expansion of Fe_nTi_{13-n} cluster is only caused by anharmonic vibration. At 300 K, 500 K, and 800 K, compared with unfixed total magnetic moment, the $\Delta V_T/V_0$ of Ti_{13}, Fe_1Ti_{12}, Fe_2Ti_{11}, Fe_7Ti_6, and $Fe_{12}Ti_1$ is almost the same under the condition that the total magnetic moment remains fixed as shown in Fig. 3(a), while for Fe_6Ti_7, Fe_9Ti_4, $Fe_{11}Ti_2$, and Fe_{13}, there is a significant gap between the thermal expansion of the fixed spin moment and that of the unfixed spin moment, which is caused by the magneto-volume effect, as displayed in Fig. 3(b). Meanwhile, the ΔM_T of Fe_6Ti_7, Fe_9Ti_4, $Fe_{11}Ti_2$, and Fe_{13} is rather large, as indicated in Fig. 4. Therefore, it is deemed that the rise in temperature leads to the change in Fe_nTi_{13-n} total magnetic moment, and subsequently the change in Fe_nTi_{13-n} total magnetic moment causes the variation in Fe_nTi_{13-n} volume, which is the reflection of the magneto-volume effect on microscopic atomic clusters. Hence, we have obtained the conclusion that the volume of Fe_nTi_{13-n} clusters during thermal expansion is jointly determined by the anharmonic interaction and magneto-volume effect.

3.3. Magneto-volume effect in Fe_nTi_{13-n}

The shift in the spin state of the cluster caused by thermal excitation, represented as the change in the total magnetic moment, is a prerequisite for Fe_nTi_{13-n} clusters to exhibit the magneto-volume effect on heating, as explained in Fig. 5(b). Since temperature could cause the spin state of Fe_nTi_{13-n} clusters to shift, it is significant to estimate the population of various spin state configurations at different temperatures by utilizing Boltzmann distribution law. The population (P) of various spin state configurations of Fe_nTi_{13-n} clusters as shown in Fig. 6 is calculated as follows:

$$P = \frac{e^{-\Delta E_i/kT}}{\sum e^{-\Delta E_i/kT}}, \tag{2}$$

where ΔE is the relative total energy between isomers with different spin states and the ground state, and k is the Boltzmann constant. For Ti_{13}, Fe_1Ti_{12}, Fe_2Ti_{11}, Fe_9Ti_4, and Fe_{13}, thermal excitation causes the spin state of the cluster to transition from the ground state to a lower spin state. For Fe_6Ti_7, Fe_7Ti_6, and $Fe_{11}Ti_2$, as the temperature increases, the spin state of the cluster might shift to low spin state and also to high spin state. However, the finite temperature variation does not change the spin state of $Fe_{12}Ti_1$ cluster. The local magnetic moment of each atom in Fe_nTi_{13-n} clusters at different temperatures is also calculated, as shown in Fig. S4. Generally speaking, the spin states of Fe atoms and Ti atoms in Fe–Ti clusters are consistent with the change trend of the overall cluster spin states with the temperature increasing. The results drawn from the population calculation are essentially consistent with the change of the total magnetic moment obtained in the thermal expansion simulation in Fig. 4, which further illustrates the rationality of the transition in the cluster spin state caused by thermal excitation. Meanwhile, the shift in the spin state caused by thermal excitation is a prerequisite for the magneto-volume effect of Fe_nTi_{13-n} clusters during thermal expansion.

To study the effect of the total magnetic moment on the cluster volume, the magneto-volume (V_M) is defined as the volume when the total magnetic moment is M, which is varied by the change in total magnetic moment of clusters on heating. Combining Fe_nTi_{13-n} volumes at 300 K, 500 K, and 800 K obtained by the FSM thermal relaxation simulation, the V_M of Fe_nTi_{13-n} clusters can be calculated as follows:

$$V_M = \Delta V_M + V_0, \quad \Delta V_M = V_{T,M} - V_{T,M_0}, \tag{3}$$

where ΔV_M denotes the volume difference between magneto-volume and ground state volume, $V_{T,M}$ denotes the Fe_nTi_{13-n} volume when the temperature is T and the total magnetic moment is M, and V_{T,M_0} denotes the Fe_nTi_{13-n} volume when the temperature is T and the total magnetic moment is M_0. It has been discovered that Fe_6Ti_7, Fe_9Ti_4, $Fe_{11}Ti_2$, and Fe_{13}

have considerable magneto-volume effect during thermal expansion, so the relative volume (ΔV) and relative total energy (ΔE) of their isomers with different spin states in comparison to the ground state are displayed in Fig. 7. The ΔV_M induced by the magneto-volume effect is also plotted in Fig. 7. For Fe_6Ti_7 and Fe_{13}, the ΔV_M roughly matches the ΔV caused by changing the spin state. For Fe_9Ti_4 and $Fe_{11}Ti_2$, the ΔV_M is slightly different with the ΔV. In other words, if the total magnetic moment of Fe_nTi_{13-n} in thermal expansion is known, the ΔV_M can be roughly estimated from the ΔV according to Fig. 7. This is sufficient to demonstrate the logic of the magneto-volume effect during thermal expansion and approximately calculate the magnitude of the magneto-volume produced by the magneto-volume effect in Fe_nTi_{13-n} clusters.

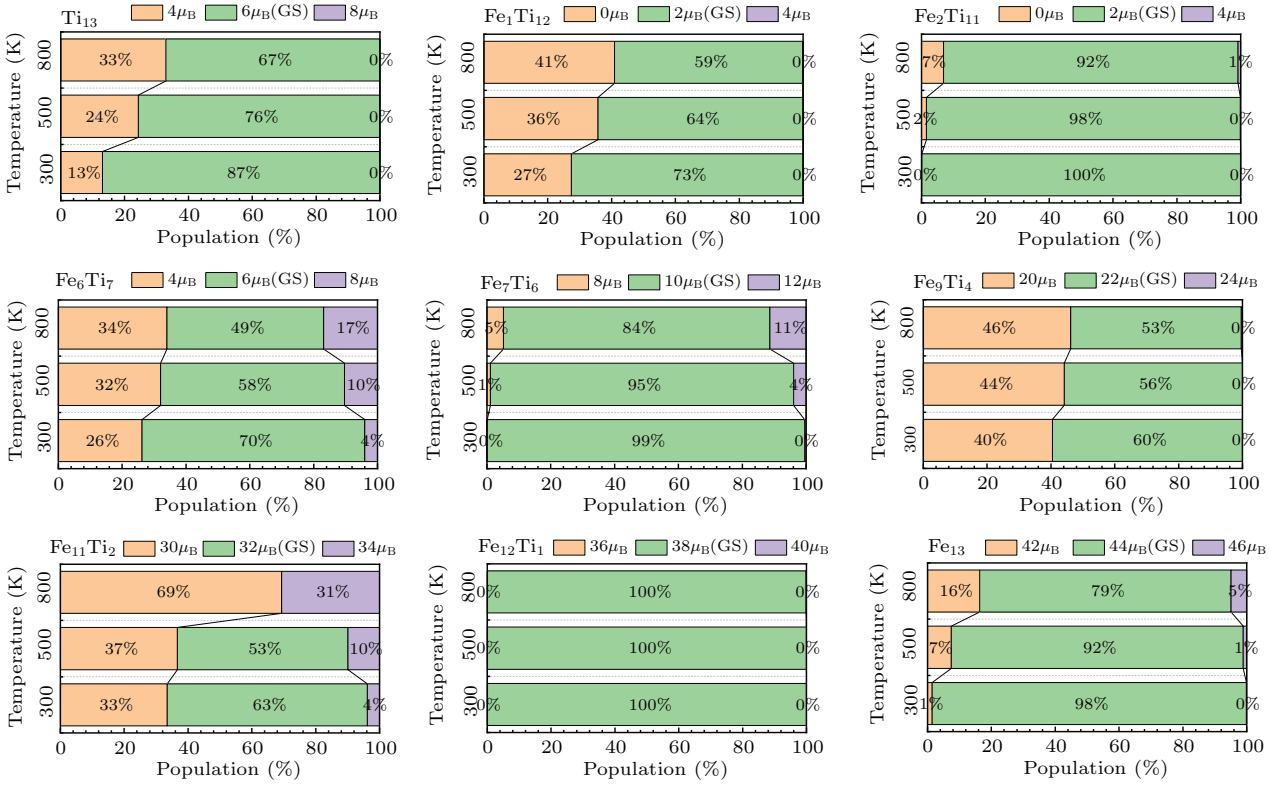


Fig. 6. Population of various spin state configurations of Fe_nTi_{13-n} clusters at 300 K, 500 K, and 800 K.

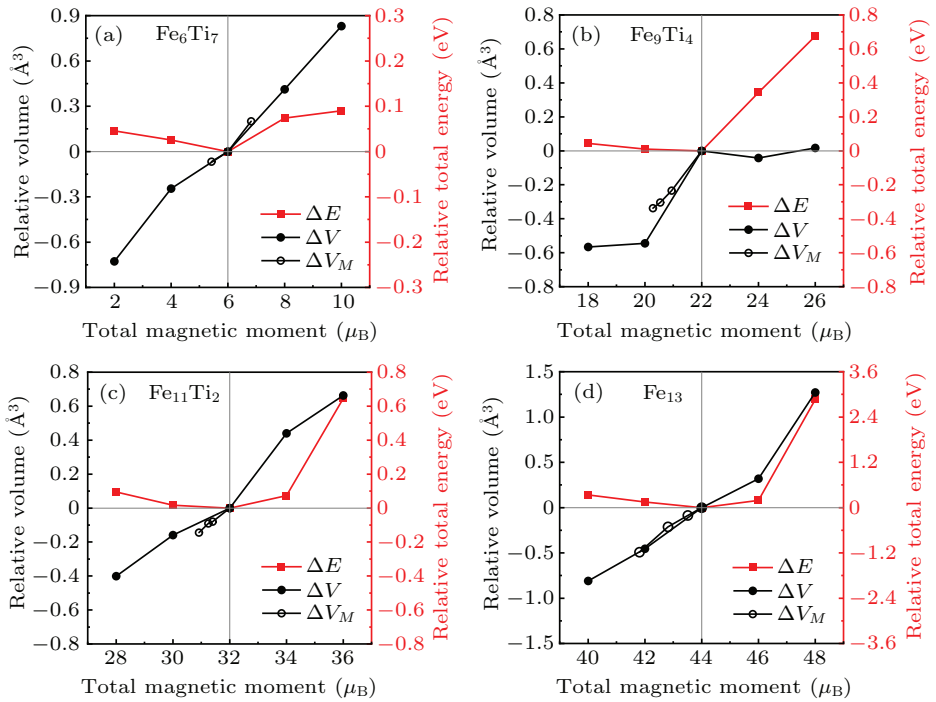


Fig. 7. The relative volume (ΔV) and relative total energy (ΔE) of isomers with different spin sates in comparison to the ground state of Fe_nTi_{13-n}. The horizontal gray solid line indicates that the relative value is 0, and the vertical gray solid line indicates that the total magnetic moment is M_0.

The moment-volume instability is the reason why the 3d alloy cluster system exhibits the magneto-volume effect.[59] This is also illustrated by our above DFT computational studies. For the magnetic metal cluster system, the existence of temperature-excited spin metastable state is a necessary condition for the cluster to exhibit the magneto-volume effect. At the same time, there is a large gap between the volume of the spin metastable state and the volume of the ground state, which leads to the obvious magneto-volume effect of the cluster during thermal expansion. To further explore the magneto-volume effect in Fe_nTi_{13-n}, the energy contour map with respect to the volume and the total magnetic moment is created in Fig. 8. The density of the contour line reflects the pace of total energy change. If $V_{T,M}$, V_{T,M_0}, and V_M are regarded as vectors starting from the ground state point (the intersection of the M_0 axis and the V_0 axis), then $\boldsymbol{V}_{T,M}$, $\boldsymbol{V}_{T,M_0}$, and $\boldsymbol{V}_M$ naturally meet the parallelogram law, which can be described by vector equation

$$\boldsymbol{V}_{T,M} = \boldsymbol{V}_{T,M_0} + \boldsymbol{V}_M. \tag{4}$$

Hence, the vector diagrams of $\boldsymbol{V}_{T,M}$, $\boldsymbol{V}_{T,M_0}$, and $\boldsymbol{V}_M$ at 300 K, 500 K, and 800 K are plotted in Fig. 8. In the energy contour map, each point contains the information of the volume, total magnetic moment and total energy of Fe_nTi_{13-n} clusters, and the ground state point is the point with the lowest total energy of the cluster. The physical meaning of the M_0 axis is that when the total magnetic moment is M_0, the total energy changes with the volume, which conforms to the curve of potential energy changing with volume.[60] For the V_0 axis, the density of the contour lines above and below the ground state point can roughly reflect the population, that is, the change behavior of the total magnetic moment with the temperature increasing can be judged by the density of the contour lines above and below the ground state point. The energy valley (EV) direction is defined as the convex direction of the contour lines, which is also the direction where the total energy changes relatively slowly. There are always two EVs along the M_0 axis. One is from the ground state point along the positive direction of the volume, and the other is from the ground state point along the direction of the volume reduction, but the contour lines along the increasing direction of volume are sparser. The direction of $\boldsymbol{V}_{T,M_0}$ is the direction in which the volume increases along the M_0 axis, which is entirely due to volume expansion generated by the anharmonic interaction between atoms. Without considering the M_0 axis direction, there will be other EVs in the energy contour map of Fe_nTi_{13-n} clusters except for Fe_7Ti_6 and $Fe_{12}Ti_1$, and the vector $\boldsymbol{V}_M$ roughly points in the direction of these EVs from the ground state point, which indicates that the total magnetic moment behaviors and magneto-volume behaviors of Fe_nTi_{13-n} clusters with the temperature increasing are associated with the direction of these EVs. $\boldsymbol{V}_{T,M}$ during the actual thermal expansion is thus determined by $\boldsymbol{V}_{T,M_0}$ caused by the anharmonic interaction and $\boldsymbol{V}_M$ caused by the magneto-volume effect.

For Fe_7Ti_6 and $Fe_{12}Ti_1$, there are no other EVs in the energy contour maps without considering the EVs along the M_0 axis. For Fe_7Ti_6, the contour lines on both sides of the M_0 axis have comparable density and are somewhat dense. So, the total magnetic moment of Fe_7Ti_6 fluctuates around M_0 ($10\mu_B$) on heating. Meanwhile, the direction of $\boldsymbol{V}_M$ is almost coincident with the V_0 axis, which means the magneto-volume effect in Fe_7Ti_6 is not obvious (i.e., V_M is close to V_0). $Fe_{12}Ti_1$ has a quite similar energy contour map to Fe_7Ti_6. The difference is that the contour lines in the $Fe_{12}Ti_1$ energy contour map are extremely dense on both sides of the M_0 axis, causing the total magnetic moment of $Fe_{12}Ti_1$ always maintaining M_0 ($38\mu_B$) on heating. Hence, there is no magneto-volume effect in $Fe_{12}Ti_1$. For Fe_nTi_{13-n} ($n = 0$, 1, 2, 9, 11, 13), there is an obvious EV in energy contour maps without considering the EVs along the M_0 axis, and this EV points in the direction of decreasing total magnetic moment from the ground state point. Therefore, the total magnetic moment of these clusters decreases when the temperature rises. The direction of the EV of Ti_{13}, Fe_1Ti_{12} and Fe_2Ti_{11} approximately coincides with the V_0 axis, while that of Fe_9Ti_4, $Fe_{11}Ti_2$ and Fe_{13} is at a certain angle to the V_0 axis. As a result, the magneto-volume effect of Ti_{13}, Fe_1Ti_{12} and Fe_2Ti_{11} is not obvious on heating, while that of Fe_9Ti_4, $Fe_{11}Ti_2$ and Fe_{13} is obvious. For Fe_6Ti_7, there are two EVs in the energy contour map without considering the EVs along the M_0 axis, and these two EVs are located on the upper and lower sides of the M_0 axis, and both form a certain angle with the V_0 axis. Thus, the total magnetic moment of Fe_6Ti_7 fluctuates around the M_0 ($6\mu_B$) with the temperature increasing, producing an obvious magneto-volume. At different temperature, the total magnetic moment change behavior for Fe_6Ti_7 is diverse. At 300 K, the average total magnetic moment of Fe_6Ti_7 is larger than M_0, resulting in V_M to be larger than V_0. Because the average total magnetic moment of Fe_6Ti_7 is smaller than M_0 at 800 K, V_M is smaller than V_0. The average total magnetic moment of Fe_6Ti_7 is close to M_0 at 500 K, so V_M is close to V_0.

After the above discussion, in addition to the FSM-AIMD calculation, the magneto-volume effect of Fe_nTi_{13-n} clusters during thermal expansion can also be analyzed through the energy contour maps. In shorts, in the energy contour maps (without considering the EVs along the M_0 axis), if there are no other EVs, or the direction of the EVs coincides with the V_0 axis, the clusters will exhibit an insignificant magneto-volume effect on heating. If the direction of the EVs is at a certain angle to the V_0 axis, the clusters will exhibit a pronounced magneto-volume effect with the temperature increasing.

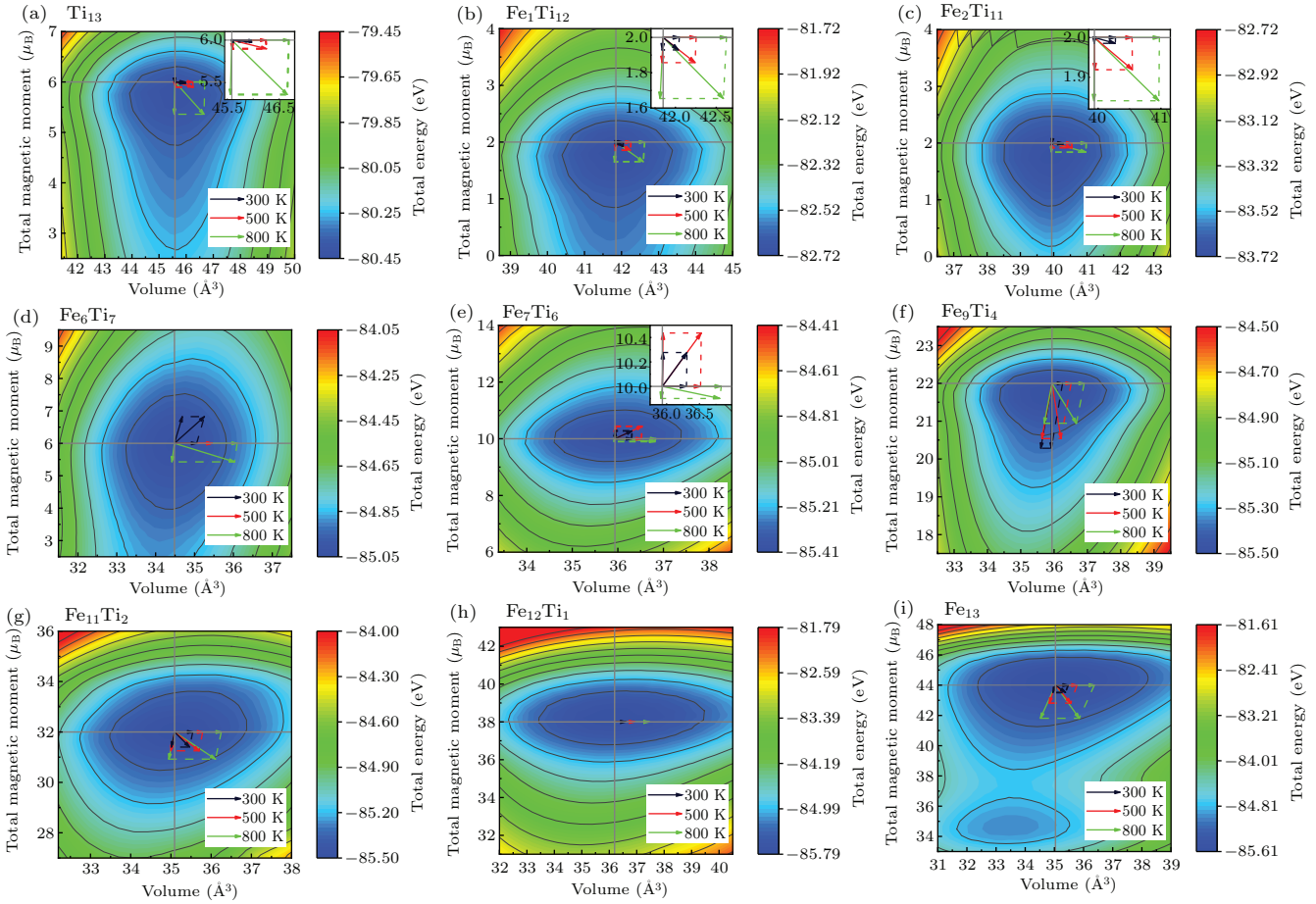


Fig. 8. The energy contour map of Fe_nTi_{13-n}. The horizontal and vertical gray solid lines represent the M_0 axis and the V_0 axis, respectively. The vector diagrams of $\boldsymbol{V}_{T,M}$, $\boldsymbol{V}_{T,M_0}$, and $\boldsymbol{V}_M$ at 300 K, 500 K, and 800 K are plotted. A partial enlarged view of the volume vector diagram is drawn in the upper right corner of (a), (b), (c), and (e).

4. Conclusion

In summary, the ground state and characteristics of Fe_nTi_{13-n} clusters have been obtained by the first principles calculations, as well as the volume and the total magnetic moment of Fe_nTi_{13-n} at different temperatures. The main conclusions can be made as follows. (1) The magneto-volume effect of Fe_6Ti_7, Fe_9Ti_4, $Fe_{11}Ti_2$, and Fe_{13} is considerable during thermal expansion, while that of Ti_{13}, Fe_1Ti_{12}, Fe_2Ti_{11}, Fe_7Ti_6, and $Fe_{12}Ti_1$ is not obvious. (2) The volume of Fe_nTi_{13-n} clusters during thermal expansion is jointly determined by the anharmonic interaction and magneto-volume effect. (3) The shift in the spin state caused by thermal excitation is a prerequisite for Fe_nTi_{13-n} clusters to exhibit the magneto-volume effect during thermal expansion. Meanwhile, if the total magnetic moment of Fe_nTi_{13-n} during thermal expansion is known, the ΔV_M induced by the magneto-volume effect can be roughly estimated from the ΔV. (4) Finally, the energy contour map can be applied to analyze the total magnetic moment behaviors and volume behaviors of clusters during thermal expansion and determine the magneto-volume effect of Fe_nTi_{13-n} clusters.

Our findings highlight the importance of the magneto-volume effect on the volume change of Fe_nTi_{13-n} clusters during thermal expansion, and contribute to a better understanding of the magneto-volume effect mechanism at the cluster scale. And, it will be feasible to develop controlled thermal expansion nanodevices using the magneto-volume effect mechanism during thermal expansion.

Acknowledgements

We are grateful for the useful discussions with Chengrui Fu. We would like to acknowledge the support from the National Natural Science Foundation of China (Grant No. 52171038) as well as key R&D projects in Shandong Province (Grant No. 2021SFGC1001). This work is also supported by the Special Funding in the Project of the Taishan Scholar Construction Engineering and the program of Jinan Science and Technology Bureau (Grant No. 2020GXRC019) as well as new material demonstration platform construction project from Ministry of Industry and Information Technology of China (Grant No. 2020-370104-34-03-043952-01-11).

Data availability statement

The data that support the findings of this study are available from the corresponding author upon reasonable request.

References

[1] van Schilfgaarde M, Abrikosov I A and Johansson B 1999 *Nature* **400** 46
[2] Song Y Z, Shi N K, Deng S Q, Xing X R and Chen J 2021 *Prog. Mater. Sci.* **121** 100835
[3] Guillaume C E 1904 *Nature* **71** 134
[4] Moruzzi V L 1990 *Phys. Rev. B* **41** 6939
[5] Ekholm M and Abrikosov I A 2011 *Phys. Rev. B* **84** 104423
[6] Akai H and Dederichs P H 1993 *Phys. Rev. B* **47** 8739
[7] Abrikosov I A, Kissavos A E, Liot F, Alling B, Simak S I, Peil O and Ruban A V 2007 *Phys. Rev. B* **76** 014434
[8] Liot F and Abrikosov I A 2009 *Phys. Rev. B* **79** 014202
[9] Korenman V and Wyman B 1981 *Phys. Rev. B* **24** 5413
[10] Rao Z Y, Cakir A, Ozgun O, Ponge D, Raabe D, Li Z M and Acet M 2021 *Phys. Rev. Mater.* **5** 044406
[11] Iikubo S, Kodama K, Takenaka K, Takagi H, Takigawa M and Shamoto S 2008 *Phys. Rev. Lett.* **101** 205901
[12] Iikubo S, Kodama K, Takenaka K, Takagi H and Shamoto S 2008 *Phys. Rev. B* **77** 020409
[13] Takenaka K and Takagi H 2005 *Appl. Phys. Lett.* **87** 261902
[14] Takenaka K, Ichigo M, Hamada T, Ozawa A, Shibayama T, Inagaki T and Asano K 2014 *Sci. Technol. Adv. Mater.* **15** 015009
[15] Cowley R A 1963 *Adv. Phys.* **12** 421
[16] Wallace D C 1965 *Phys. Rev.* **139** A877
[17] Yokoyama T and Eguchi K 2013 *Phys. Rev. Lett.* **110** 075901
[18] Khmelevskyi S, Turek I and Mohn P 2003 *Phys. Rev. Lett.* **91** 037201
[19] Khmelevskyi S and Mohn P 2010 *Phys. Rev. B* **82** 134402
[20] Huang R, Liu Y, Fan W, Tan J, Xiao F, Qian L and Li L 2013 *J. Am. Chem. Soc.* **135** 11469
[21] Song Y, Sun Q, Yokoyama T, Zhu H, Li Q, Huang R, Ren Y, Huang Q, Xing X and Chen J 2020 *J. Phys. Chem. Lett.* **11** 1954
[22] Wang C, Chu L, Yao Q, Sun Y, Wu M, Ding L, Yan J, Na Y, Tang W, Li G, Huang Q and Lynn J W 2012 *Phys. Rev. B* **85** 220103
[23] Guo X G , Lin J C, Tong P, Wang M, Wu Y, Yang C, Song B, Lin S, Song W H and Sun Y P 2015 *Appl. Phys. Lett.* **107** 202406
[24] Song Y, Chen J, Liu X, Wang C, Zhang J, Liu H, Zhu H, Hu L, Lin K, Zhang S and Xing X 2018 *J. Am. Chem. Soc.* **140** 602
[25] Li B, Luo X H, Wang H, Ren W J, Yano S, Wang C W, Gardner J S, Liss K D, Miao P, Lee S H, Kamiyama T, Wu R Q, Kawakita Y and Zhang Z D 2016 *Phys. Rev. B* **93** 224405
[26] Li L F, Tong P, Zou Y M, Tong W, Jiang W B, Jiang Y, Zhang X K, Lin J C, Wang M, Yang C, Zhu X B, Song W H and Sun Y P 2018 *Acta Mater.* **161** 258
[27] Poteryaev A I, Skorikov N A, Anisimov V I and Korotin M A 2016 *Phys. Rev. B* **93** 205135
[28] Song Y, Sun Q, Xu M, Zhang J, Hao Y, Qiao Y, Zhang S, Huang Q, Xing X and Chen J 2020 *Mater. Horizons* **7** 275
[29] Fu C, Huang J, Jiang Y and Li H 2022 *J. Phys. Chem. Lett.* **13** 6644
[30] Kohn W and Sham L J 1965 *Phys. Rev.* **140** A1133
[31] Hohenberg P and Kohn W 1964 *Phys. Rev. B* **136** B864
[32] Kresse G and Hafner J 1993 *Phys. Rev. B* **48** 13115
[33] Kresse G and Furthmuller J 1996 *Phys. Rev. B* **54** 11169
[34] Perdew J P, Chevary J A, Vosko S H, Jackson K A, Pederson M R, Singh D J and Fiolhais C 1992 *Phys. Rev. B* **46** 6671
[35] Perdew J P, Burke K and Ernzerhof M 1996 *Phys. Rev. Lett.* **77** 3865
[36] Blochl P E 1994 *Phys. Rev. B* **50** 17953
[37] Nose S 1984 *J. Chem. Phys.* **81** 511
[38] Hoover W G 1985 *Phys. Rev. A* **31** 1695
[39] Baletto F and Ferrando R 2005 *Rev. Mod. Phys.* **77** 371
[40] Pannetier J, Bassasalsina J, Rodriguezcarvajal J and Caignaert V 1990 *Nature* **346** 343
[41] Jones R O 1993 *J. Chem. Phys.* **99** 1194
[42] Wang L L and Johnson D D 2007 *Phys. Rev. B* **75** 235405
[43] Piotrowski M J, Piquini P and Da Silva J L F 2010 *Phys. Rev. B* **81** 155446
[44] Bobadova-Parvanova P, Jackson K A, Srinivas S and Horoi M 2002 *Phys. Rev. B* **66** 195402
[45] Ma Q M, Xie Z, Wang J, Liu Y and Li Y C 2007 *Solid State Commun.* **142** 114
[46] Kim E, Mohrland A, Weck P F, Pang T, Czerwinski K R and Tomanek D 2014 *Chem. Phys. Lett.* **613** 59
[47] Wang S Y, Yu J Z, Mizuseki H, Yan J A, Kawazoe Y and Wang C Y 2004 *J. Chem. Phys.* **120** 8463
[48] Wang S Y, Duan W, Zhao D L and Wang C Y 2002 *Phys. Rev. B* **65** 165424
[49] Yuan H K, Chen H, Kuang A L, Tian C L and Wang J Z 2013 *J. Chem. Phys.* **139** 034314
[50] Alvarado-Leyva P G, Aguilera-Granja F, Balbas L C and Vega A 2013 *Phys. Chem. Chem. Phys.* **15** 14458
[51] Purdum H, Montano P A, Shenoy G K and Morrison T 1982 *Phys. Rev. B* **25** 4412
[52] Doverstal M, Lindgren B, Sassenberg U, Arrington C A and Morse M D 1992 *J. Chem. Phys.* **97** 7087
[53] Dieguez O, Alemany M M G, Rey C, Ordejon P and Gallego L J 2001 *Phys. Rev. B* **63** 205407
[54] Singh R and Kroll P 2008 *Phys. Rev. B* **78** 245404
[55] de Heer W A, Milani P and Chtelain A 1990 *Phys. Rev. Lett.* **65** 488
[56] Billas I M, Chatelain A and de Heer W A 1994 *Science* **265** 1682
[57] Apsel S E, Emmert J W, Deng J and Bloomfield L A 1996 *Phys. Rev. Lett.* **76** 1441
[58] Moruzzi V L and Marcus P M 1988 *Phys. Rev. B* **38** 1613
[59] Wassermann E F 1991 *J. Magn. Magn. Mater.* **100** 346
[60] Sleight A 2003 *Nature* **425** 674